Structural transformations in the In_5Bi_3 compound under high pressure

2002 J. Phys.: Condens. Matter 14 407

(http://iopscience.iop.org/0953-8984/14/3/310)

INSTITUTE OF PHYSICS PUBLISHING JOURNAL OF PHYSICS: CONDENSED MATTER

J. Phys.: Condens. Matter **14** (2002) 407–414 PII: S0953-8984(02)29270-X

Structural transformations in the In_5Bi_3 compound under high pressure

Olga Degtyareva[1,3] **and Valentina F Degtyareva**[2]

[1] Department of Physics and Astronomy, The University of Edinburgh, Edinburgh EH9 3JZ, UK
[2] Institute of Solid State Physics, Chernogolovka, Moscow District, 142432, Russia

Received 28 September 2001
Published 21 December 2001
Online at stacks.iop.org/JPhysCM/14/407

Abstract

The compound In_5Bi_3 decomposes at pressure 15 GPa and temperature 150 °C into two phases of different compositions. Each phase represents a tetragonal distortion of the body-centred cubic phase, one with axial ratio $c/a > 1$ and the other with $c/a < 1$. These phases follow the Bain path—a tetragonal distortion of the cubic structure on the way from face-centred cubic to body-centred cubic, observed for tetragonal phases of In and Sn alloys as a function of composition (or electron concentration) at ambient and high pressure. Ambient-pressure stoichiometic compounds in the In–Bi alloy system are replaced under pressure by a sequence of metallic random phases with the structure determined by the electron concentration.

1. Introduction

The In_5Bi_3 compound crystallizes in the tetragonal structure with lattice parameters $a = 8.544$ Å and $c = 12.68$ Å, with 32 atoms in the unit cell, space group $I4/mcm$ [1]. The atomic arrangement in this compound consists of square-triangle 3^2434 nets in ab-planes and of square nets of atoms over the cell corners and over the base [2]. The structure is site ordered with the position occupation as follows: Bi at 4a (0, 0, 0.25), In at 4c (0, 0, 0), Bi at 8h $(x, x+1/2, 0)$ with $x = 0.343$, and In at 16ℓ $(x, x+1/2, z)$ with $x = 0.144$ and $z = 0.168$.

The In_5Bi_3 structure is related to a recently determined *incommensurate* structure of Bi III [3] and can be viewed as a *commensurate* approximant for Bi III-type structure. The interest in high-pressure studies of the In_5Bi_3 compound is due to similarities in the atomic arrangement with Bi III. In this paper the results on high-pressure structural transformations of the In_5Bi_3 compound are presented.

[3] On leave from: The Institute of Solid State Physics, Chernogolovka, Moscow District, 142432, Russia.

0953-8984/02/030407+08$30.00

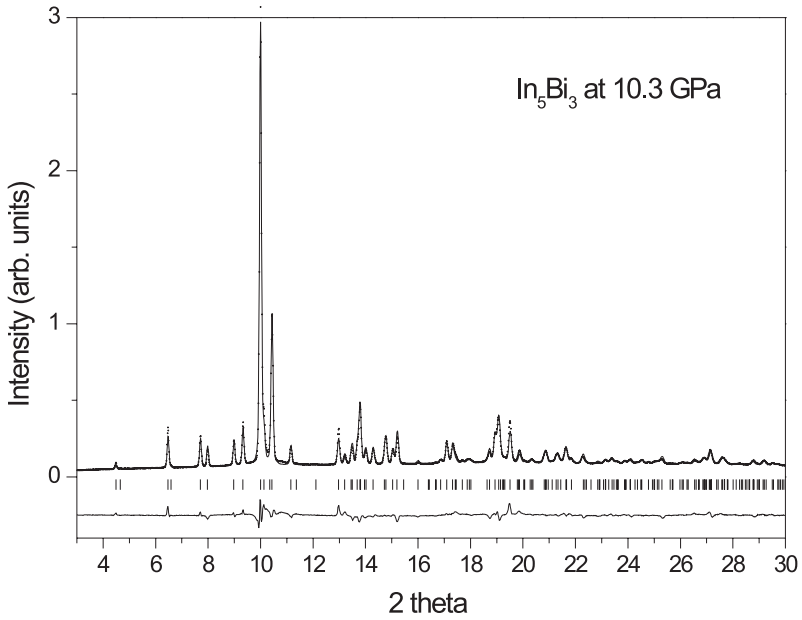

Figure 1. The integrated profile from In_5Bi_3 at 10.3 GPa (crosses) and a Rietveld refinement fit (curve). The tick marks below the profile show the peak positions of the tI32, $I4/mcm$, structure. The lower curve is the difference between the observed and calculated profiles.

2. Experimental details

Experiments were carried out on an alloy of composition In—37.5 at.% Bi obtained by melting, in an evacuated silica capsule, appropriate amounts of In and Bi of 5N purity. The composition was selected in accordance with the known phase diagram of the In–Bi alloy system [4]. The x-ray diffraction pattern of the alloy under ambient conditions corresponds to the structure of the In_5Bi_3 compound.

Angle-dispersive powder diffraction data were collected on station 9.1 at the Synchrotron Radiation Source (SRS), Daresbury Laboratory, using a diamond-anvil cell and an image-plate area detector, with a wavelength of 0.4654(1) Å [5]. The gasket hole was filled with a piece of sample, a 4:1 methanol:ethanol mixture as a pressure medium, and a small chip of ruby for the pressure measurement. The 2D images were integrated azimuthally, and structural information was obtained by Rietveld refinement of the integrated profiles using the program GSAS [6].

The experiment was performed in two runs of pressure loading: at room temperature and with heating under pressure.

3. Results

Structural studies of the In_5Bi_3 compound under pressure at room temperature show that this compound remains stable up to 25 GPa. A Rietveld fit to the integrated profile obtained from the In_5Bi_3 sample at 10.3 GPa is shown in figure 1. The lattice parameters at these pressures are $a = 8.0894(2)$ Å and $c = 11.8760(6)$ Å, with atomic volume $V = 24.29(2)$ Å^3 and axial ratio $c/a = 1.468$. The refined atomic positions are $x_1 = 0.3472(2)$ for Bi at 8h and $x_2 = 0.1488(3)$ and $z = 0.1670(3)$ for In at 16ℓ, which are very close to the values at ambient pressure. The

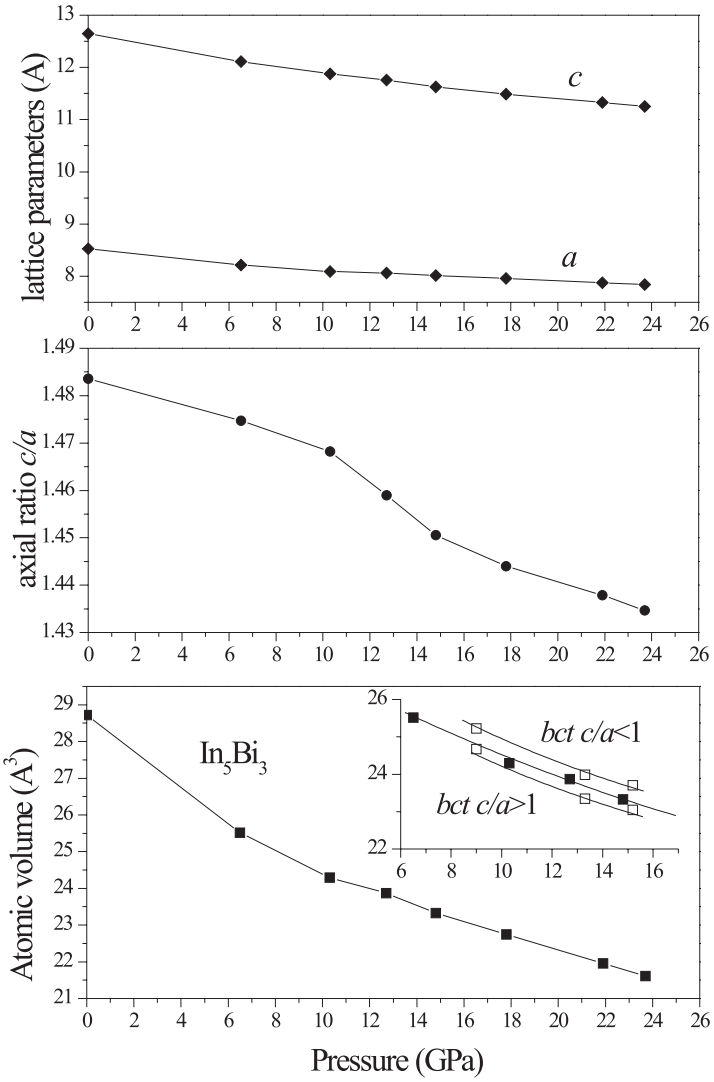

Figure 2. Variations of lattice parameters, axial ratio, and atomic volume with pressure for the In_5Bi_3 compound at room temperature. The inset shows the atomic volume for the bct, $c/a > 1$ and bct, $c/a < 1$ phases (open squares) in the alloy annealed at 15 GPa, 150 °C, 4 h, together with the atomic volume of the In_5Bi_3 compound without annealing (solid squares).

R-factors are $wR_p = 7.0\%$, $R_p = 5.1\%$, and $\chi^2 = 0.6$ for 17 variables. Variations of the lattice parameters and the atomic volume with pressure are presented in figure 2. The axial ratio decrease with pressure increase corresponds to higher compression along c comparing to a. A remarkable bend in the c/a variation versus pressure occurs above 10 GPa. Diffraction peaks above this pressure become very broad, and therefore in the next run the In_5Bi_3 sample was annealed at 15 GPa and 150 °C for 4 h.

The diffraction pattern after annealing looks completely different, displaying that a phase transition has occurred. The most remarkable feature of this pattern is the absence of the low-angle diffraction peaks seen in figure 3. This implies a relatively short lattice axis in the newly

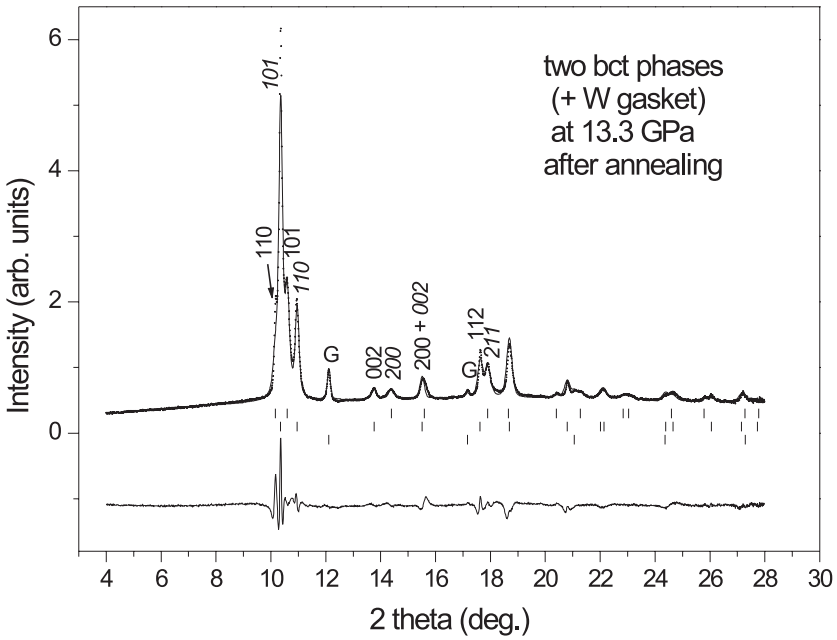

Figure 3. The integrated profile from the In_5Bi_3 alloy at 13.3 GPa (crosses) after decomposition and a Rietveld refinement fit (curve). The tick marks below the profile show the peak positions of the bct, $c/a < 1$ (upper) and bct, $c/a > 1$ (middle) phases and of the W gasket (lower). Below the tick marks is the difference between the observed and calculated profiles. Indices of some diffraction peaks are indicated as upright *hkl* for the bct, $c/a < 1$ phase and as sloping *hkl* for the bct, $c/a > 1$ phase. 'G' indicates the strongest diffraction peaks of the gasket material.

formed alloy structural state. No solution was found by assuming this state to be a single-phase state. An attempt to account for this pattern by a two-phase mixture resulted in a solution with two tetragonal phases. Both phases are body-centred tetragonal (bct) with two atoms in the cell, occupying the 2a position of space group $I4/mmm$, but differing in axial ratio. These structures represent small tetragonal distortions of a body-centred cubic (bcc) structure. One with the axial ratio $c/a = 0.92$ is assigned here as bct, $c/a < 1$. The other structure with $c/a = 1.13$ can be considered as a tetragonal distortion intermediate between a bcc ($c/a = 1$) and a fcc ($c/a = 1.41$) structure. This structure is assigned here as bct, $c/a > 1$.

The pressure in the cell with this sample has been decreased from 15 GPa, and both tetragonal phases have been observed to be stable at least down to 9 GPa. On pressure release, the initial In_5Bi_3 compound was recovered, indicating the reversibility of the observed transformation.

A Rietveld refinement of the integrated profile for the sample at 15.2 GPa, assuming a mixture of two tetragonal phases, is shown in figure 3. The lattice parameters have been determined from a least-square fit of d-spacings and were fixed in the Rietveld refinement. The lattice parameters for bct, $c/a < 1$ are $a = 3.715(3)$ Å, $c = 3.426(7)$ Å, $c/a = 0.923$; and for bct, $c/a > 1$ they are $a = 3.447(2)$ Å, $c = 3.883(3)$ Å, $c/a = 1.126$. The amount of the bct, $c/a > 1$ phase is two times greater than the amount of the bct, $c/a < 1$ phase. The R-factors of the fit are $wR_p = 5.6\%$, $R_p = 4\%$, and $\chi^2 = 0.2$ for 16 variables. The remaining discrepancies between the observed and calculated profiles arise from stresses due to the non-hydrostatic conditions causing broadness of the lines and deviation of the diffraction peak positions from the calculated values.

Table 1. Structural characteristics of phases in the In_5Bi_3 alloy at pressure $P = 15.2$ GPa, obtained after annealing at 150 °C.

Phase	a (Å)	c (Å)	c/a (bct)	V_{at} (Å^3)	Composition (at.% Bi)	Electron concentration (electrons/atom)
bct, $c/a < 1$	3.715(3)	3.426(7)	0.923(2)	23.67(6)	∼44	3.88
bct, $c/a > 1$	3.447(2)	3.883(3)	1.126(1)	23.07(3)	∼34	3.68

The axial ratio, for both these phases, does not show any significant variation within the pressure range 15–9 GPa. The atomic volumes of these phases have slightly different values, as shown in figure 2 (inset): one is above and the other is below that of the In_5Bi_3 compound. This observation implies that the In_5Bi_3 compound decomposes into two phases of different composition. The difference in composition corresponds to about 10 at.%. This estimate follows from Vegard's law for alloy solid solutions. The compositions are estimated as ∼34 at.% Bi for bct, $c/a > 1$ and ∼44 at.% Bi for bct, $c/a < 1$. As the amount of bct, $c/a > 1$ phase in the pattern is greater than that of bct, $c/a < 1$, the phase bct, $c/a > 1$ is shifted in composition less than the phase bct, $c/a < 1$ from the initial In_5Bi_3 content. The compositions of these two coexisting phases do not vary over the range 15–9 GPa.

Both phases seem to be site disordered, because no extra peaks that could indicate possible order in these alloy phases were observed. Structural details for these two phases are summarized in table 1.

4. Discussion

It is interesting to compare these tetragonal phases with other similar phases known in In-based alloys [7]. The element In has a tetragonal structure at ambient pressure, which is a small distortion of a fcc structure with an axial ratio $c/a = 1.07$ in the face-centred tetragonal (fct) setting [8]. A tetragonal distortion of phases caused by alloying of In with neighbouring elements in the periodic table depends on the average number of valence electrons per atom, or electron concentration. Figure 4 shows a representative plot for axial ratios of the tetragonal phases for In–Sn and related alloys with neighbouring elements as a function of electron concentration.

On alloying In with the divalent elements Hg and Cd, the axial ratio decreases, and changes discontinuously down to $c/a = 1$ at $n < 2.94$, where the fcc phase is stable [7]. On alloying of In with elements of higher valency Pb, Sn, and Bi, the axial ratio of the tetragonal phase increases to the value $c/a = 1.10$ (fct, $c/a > 1$). At higher concentrations, $n > 3.15$, the axial ratio makes a jump to the values <1 (fct, $c/a < 1$ or bct, $c/a > 1$). The solid line represents axial ratio values as a function of electron concentration for the In alloys with Sn, Pb, and Bi at ambient pressure, involving data on equilibria and metastable ('splat-cooling') phases [7, 9]. The dashed curve shows axial ratio values for the In–Sn, In–Pb alloys under pressure [10]. These data, lying between $c/a = 1$ and $1/\sqrt{2}$, represent the Bain path—a tetragonal distortion of the cubic structure on the way from fcc to bcc.

The bcc structure is realized in the heavy group IV elements Sn and Pb [11, 12]. A tetragonal distortion occurs in Sn under pressure before the transition to bcc structure, with the axial ratio reaching $c/a = 0.96$ (in the fct setting $c/a = 0.68$) [11]. Similar tetragonal distortion of bcc structure has been observed in the isoelectronic compound InBi under pressure, with the same axial ratio [13]. This value can be read from figure 4 at the electron concentration

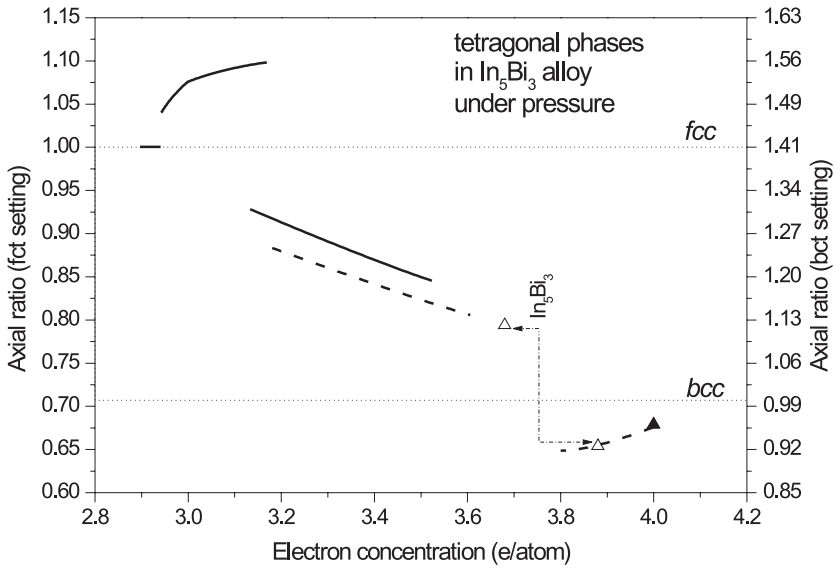

Figure 4. A representative plot of axial ratios of the tetragonal phases for In–Sn and related alloys as a function of electron concentration. Dotted horizontal lines correspond to c/a values for fcc and bcc structures. The solid curves represent average values of axial ratios for In alloys with Cd, Hg, Sn, Pb, and Bi at ambient pressure, whether stable [7] or metastable [9]. The dashed curves represent axial ratios observed at high pressure for the alloys In–Sn, In–Pb (middle branch), and Sn–Hg, Sn–In, In–Bi (lower branch) [10, 13–15]. The dot–dashed vertical line indicates the position of the initial In_5Bi_3 compound, and horizontal arrows indicate its decomposition into two tetragonal phases with different c/a ratios, denoted by open triangles. The solid triangle denotes the high-pressure bct phase in InBi [13].

$n = 4$. The dashed curve extending from this point towards lower electron concentration represents tetragonal distortions in the Sn-rich alloys with In and Hg under pressure [14, 15].

The In_5Bi_3 compound ($n = 3.75$), indicated by the vertical dot–dashed curve in figure 4, decomposes under pressure into two tetragonal phases, bct, $c/a > 1$ and bct, $c/a < 1$ with estimated compositions corresponding to n-values of 3.68 and 3.88, respectively.

The present result on In–Bi thus gives us two more examples of tetragonal phases, as plotted in figure 4. One of them, bct, $c/a < 1$, belongs to the lower (right) branch of the plot of c/a versus n. This phase can be considered as an extension of the tetragonal phase observed in InBi under pressure with the range of compositions from 44 to at least 50 at.% Bi. The axial ratio increases from $c/a = 0.92$ to 0.96 as the electron concentration n increases from 3.88 to 4, showing a correlation between the tetragonal distortion and the average number of valence electrons in an alloy as discussed in [13, 14].

The other tetragonal phase, bct, $c/a > 1$, belongs to the middle branch of the plot. The data point at $c/a = 0.80$ (in the fct setting) and $n = 3.68$ agrees with the dashed curve, representing high-pressure data on the In alloys [10]. This bct, $c/a > 1$ phase can be related to the phase stability region of the fct, $c/a < 1$ phase located at 8–12 at.% Bi ($n \sim 3.16$–3.24) on the equilibrium phase diagram (figure 5), and extended to 26 at.% Bi ($n \sim 3.52$) in 'splat-cooling' experiments on In–Bi alloys [9].

The phase transformations under pressure in the In_5Bi_3 alloy thus reveal an example of decomposition of a stoichiometric compound into two phases of different compositions, which is allowed by the Gibbs phase rule for a two-component system. Without heating,

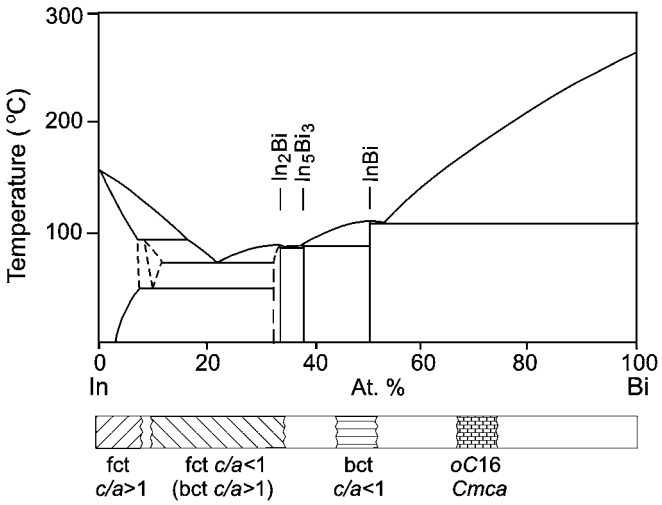

Figure 5. T–x phase diagram for In–Bi alloy systems at ambient pressure [4]. The plot below the diagram shows schematically the phase sequence and proposed regions of phase stability under pressure. The boundary between fct, $c/a > 1$ and fct, $c/a < 1$ phases is shown, relating to ambient-pressure data on stable and metastable phases discussed in the text.

decomposition was not observed because of the hindrance of the diffusion. The sample retains in this case the structure of the In_5Bi_3 compound up to 25 GPa, reached in the run; however, this state should be considered as metastable.

In the In–Bi alloy system there are three intermediate compounds at ambient pressure corresponding to compositions In_2Bi, In_5Bi_3, and InBi, as shown in figure 5. On the In-rich side up to ∼7.5 at.% Bi there is In-based solid solution, the fct, $c/a > 1$ phase, followed by another fct phase with $c/a < 1$. Under high pressure all the stoichiometric compounds turn out to be unstable. Instead, a sequence of metallic random phases can be outlined with quite extended regions of stability, as shown schematically in the lower plot of figure 5. The structure of phases in this sequence is determined by the valence electron number, as for so-called Hume-Rothery phases. For the In-rich region of the In–Bi alloy system, the structural sequence under high pressure: fct, $c/a > 1 \rightarrow$ fct, $c/a < 1$ (=bct, $c/a > 1$) $\rightarrow$ bct, $c/a < 1$, is consistent with the behaviour found for the In–Sn alloy system under high pressure [16].

The phase fct, $c/a > 1$, related to In and In solid solutions with Bi, Sn, or Pb at ambient pressure [7], is stable in pure In up to pressures over 50 GPa [17].

In the Bi-rich region of the In–Bi alloy system several intermediate phases were obtained by 'pressure quenching' [18, 19], such as a simple hexagonal (sh) phase, an orthorhombically distorted sh phase, and a complex phase with $Cmca$–oC16 structure [20], related to high-pressure forms of Si and Ge [21, 22]. The region of $Cmca$–oC16 phase in the In–Bi system should be extended under certain pressure and temperature conditions up to pure Bi, because the Bi IV phase can be assigned as having a similar $Cmca$–oC16 structure [20, 23].

There is much similarity between intermetallic high-pressure phases in the In–Bi system and high-pressure forms of group IV elements, implying that these phases are not particular characteristics of certain elements or groups, but rather are common representatives of the polyvalent sp metals and alloys.

Acknowledgments

We thank Professor R J Nelmes and Dr M I McMahon for their assistance with the data collection and for stimulating discussions. This work was supported by grants from the EPSRC and facilities provided by Daresbury Laboratory. Financial support from the Russian Foundation for Basic Research by the grant No 01-02-97030 is gratefully acknowledged.

References

[1] Villars P 1997 *Pearson's Handbook, Desk Edition* (Materials Park, OH: Materials International Society)
[2] Pearson W B 1972 *The Crystal Chemistry and Physics of Metals and Alloys* (New York: Wiley)
[3] McMahon M I, Degtyareva O and Nelmes R J 2000 *Phys. Rev. Lett.* **85** 4896
[4] Massalski T B 1996 *Binary Alloy Phase Diagrams* (Metals Park, OH: American Society for Metals)
[5] Nelmes R J and McMahon M I 1994 *J. Synchrotron Radiat.* **1** 69
[6] Larson A C and Von Dreele R B 1994 General structure analysis system (GSAS) *Los Alamos National Laboratory Report* LAUR 86–748
[7] *A Handbook of Lattice Spacings and Structures of Metals and Alloys* 1964 vol 1, ed W B Pearson (Oxford: Pergamon)
A Handbook of Lattice Spacings and Structures of Metals and Alloys 1967 vol 2, ed W B Pearson (Oxford: Pergamon)
[8] Villars P and Calvert L D 1985 *Pearson's Handbook of Crystallographic Data for Intermetallic Phases* (Metals Park, OH: American Society for Metals)
[9] Giessen B C, Morris M and Grant N J 1967 *Trans. Metall. Soc. AIME* **239** 883
[10] Degtyareva O, Degtyareva V F, Porsch F and Holzapfel W B 2001 *J. Phys.: Condens. Matter* **13** 7295
[11] Olijnyk H and Holzapfel W B 1984 *J. Physique Coll.* **45** C8 153
[12] Vanderborgh C A, Vohra Y K, Xia H and Ruoff A L 1990 *Phys. Rev.* B **41** 7338
[13] Degtyareva V F, Winzenick M and Holzapfel W B 1998 *Phys. Rev.* B **57** 4975
[14] Degtyareva V F, Degtyareva O, Winzenick M and Holzapfel W B 1999 *Phys. Rev.* B **59** 6058
[15] Degtyareva V F, Degtyareva O, Holzapfel W B and Takemura K 2000 *Phys. Rev.* B **61** 5823
[16] Degtyareva O, Degtyareva V F, Porsch F and Holzapfel W B 2002 *J. Phys.: Condens. Matter* **14** at press
[17] Takemura K 1991 *Phys. Rev.* B **44** 545
[18] Ponyatovskii E G and Degtyareva V F 1989 *High Pressure Res.* **1** 163
[19] Degtyareva V F and Ponyatovskii E G 1975 *Fiz. Tverd. Tela* **17** 2413 (1975 Engl. transl. *Sov. Phys.–Solid State* **17** 1593)
[20] Degtyareva V F 2000 *Phys. Rev.* B **62** 9
[21] Hanfland M, Schwarz U, Syassen K and Takemura K 1999 *Phys. Rev. Lett.* **82** 1197
[22] Takemura K, Schwarz U, Syassen K, Hanfland M, Christensen N E, Novikov D L and Loa I 2000 *Phys. Rev.* B **62** 10 603
[23] Chen J H, Iwasaki H and Kikegawa T 1997 *J. Phys. Chem. Solids* **58** 247